Neurocomputing 143 (2014) 170–181

Contents lists available at ScienceDirect

Neurocomputing

journal homepage: www.elsevier.com/locate/neucom

Identification of early-stage Alzheimer's disease using SFAM neural network

Jaouher Ben Ali [a,*], Saber Abid [a], Barrie William Jervis [b], Farhat Fnaiech [a], Cristin Bigan [c], Mircea Besleaga [d]

[a] University of Tunis, Higher School of Sciences and Techniques of Tunis, Laboratory of Signal Image and Energy Mastery (SIME), 5 Avenue Taha Hussein, PO Box 96, 1008 Tunis, Tunisia
[b] 115 Button Hill, Sheffield S11 9HG, England
[c] Ecological University of Bucharest, Bucharest, Romania
[d] Romanian Society for Clinical Neurophysiology, Bucharest, Romania

ARTICLE INFO

Article history:
Received 5 October 2013
Received in revised form
19 March 2014
Accepted 2 June 2014
Communicated by I. Bojak
Available online 17 June 2014

Keywords:
Alzheimer's disease (AD)
ARTMAP-familiarity discrimination (ARTMAP-FD)
Auditory event-related potential (AERP)
SFAM

ABSTRACT

Alzheimer's disease (AD), the most common form of dementia, is a complex and very serious nervous disease. Currently no medication is really effective against it. Even, its diagnosis and management remain challenging research problem for scientists. This paper aims towards identifying early-stage AD based upon the characteristics of the non-oscillatory independent components (ICs) of the auditory event related potential (AERP) waveforms of an oddball task for healthy and newly diagnosed AD subjects. Using 27 sensors to record P300 Evoked Potentials (EPs) as features vectors to train the simplified fuzzy adaptive resonance theory map (SFAM) neural network as a classifier, normal and AD subjects were classified with higher than 95% of success. The use of the ARTMAP-familiarity discrimination (ARTMAP-FD) shows that the separation of the two populations was achieved with high success and without any mistake.

1. Introduction

In 1906, Alois Alzheimer published the case of a patient of 51 years presented cognitive impairment, delusions and hallucinations since 1901. This patient was from Frankfurt and she called Auguste D. She died five years later the discovery of his disease (in 1906) [1]. Also through coloring, Alzheimer described the pathological lesions which are much known today as: senile plaques, neurofibrillary tangles and neuronal loss [2]. In 1910 Emil Kraepelin baptized the famous entity called "Alzheimer's disease (AD)" [2,3].

Nowadays, AD is classified as the most common form of dementia. This complex nervous disease causes loss and neuro-degeneration leading to memory impairment and other cognitive problems [3]. There is currently no known treatment that slows the progression of this disorder [4]. Thereby, the study of AD remains an interesting research field.

AD scientific research is divided into two axes:

- The creation of treatment that will cure patients or slow the progression of this disease. In this sense, experimental results are not very advanced and encouraging.
- The diagnosis to more understand this dementia which helps the investigation of the most effective treatment. In this sense, experimental results are very promising and the diagnosis of AD is possible with low error percentages, even in early-stage.

In literature, the most used techniques for AD diagnosis are:

- The brain imaging such as the Magnetic Resonance Imaging (MRI) and Positron Emission Tomography (PET) imaging. The main drawback of this technique is that it allows analyzing the behavior of AD after losing synapse and neuronal connections. Using a serial coronal MRI of an AD patient during 36 months, one can see the rapid development of the neuronal connection losses but it was really difficult to judge if it was really AD dementia [5].
- The electroencephalogram (EEG) which is a recording of electrical activity along the human scalp. In this line, digital EEG allows noninvasive analysis of cortical neuronal synchronization and more AD robust detection related EEG patterns may be obtained based on this technique [5].

As early as the first international EEG congress, held in London in 1947, it was recognized that a standard method of placement of electrodes used in electroencephalography was needed [6].

* Corresponding author. Tel.: +216 52 276 629, +336 83 769 019.
E-mail address: benalijaouher@yahoo.fr (J. Ben Ali).

http://dx.doi.org/10.1016/j.neucom.2014.06.008
0925-2312/

Currently, 256 channel EEG systems are commercially available [6]. The measurement of EEG waves requires high precision in the placement of sensors. In addition, noise elimination seems necessary. Besides, another problem is often encountered using EEG records; it is the detection of several undesired waves by a single sensor. These undesired waves are called "artifacts". All these constraints lead to converge to a single question: What is the most effective EEG methodology for AD diagnosis?

A mutual information analysis of the EEG in AD patients is presented in [7]. EEG waveforms from 16 scale electrodes in 15 AD patients and 15 healthy participants were recorded. To quantify patients and information transmitted from one time series to another, the cross-mutual information (CMI) method is used. While, auto mutual information (AMI) method is used in a time series to estimate how much on average the value of the time series can be predicted from preceding point values. Results were shown that the local CMI in AD subjects was lower than healthy participants. This proved that the EEG waveforms show potential information for the AD detection.

As shown in Fig. 1, the EEG waveform contains a number of negative (N) and positive (P) peaks. It generates electrical responses with short duration and low amplitude ($< 50\ \mu V$). The auditory event related potential (AERP) is a stimulus related response in the EEG [8]. The appeared peaks are designated N1, N2, P1, P2, and P3, where the numbers indicate the temporal order in which the peaks occur and the letters indicate the peak sign (positive or negative) [9]. For example, P3 means that the wave has positive amplitude and 3 means that it will appear 300 ms after the onset of stimulation. The use of P3 (also called P300) is highlighted and it is probably the most studied averaged ERP [8,10]. Two subtypes of P3 are frequently distinguished: the P3a originates from stimulus-driven frontal attention mechanisms during task processing, whereas P3b originates from temporal–parietal activity associated with attention and appears related to subsequent memory processing [8].

Preclinical diagnosis of AD is one of the major challenges for the prevention of this dementia. Until today, the early detection of AD remains a challenge. Prior to extensive neuronal degeneration, early stage AD detection is very helpful to limit the effect of this disease and to investigate the adequate treatments [11]. Thereby, based on EEG records, several researches have been pushed and many techniques have been used. In [12], three AD protocols were compared: eyes closed, eyes open, and counting eyes closed.

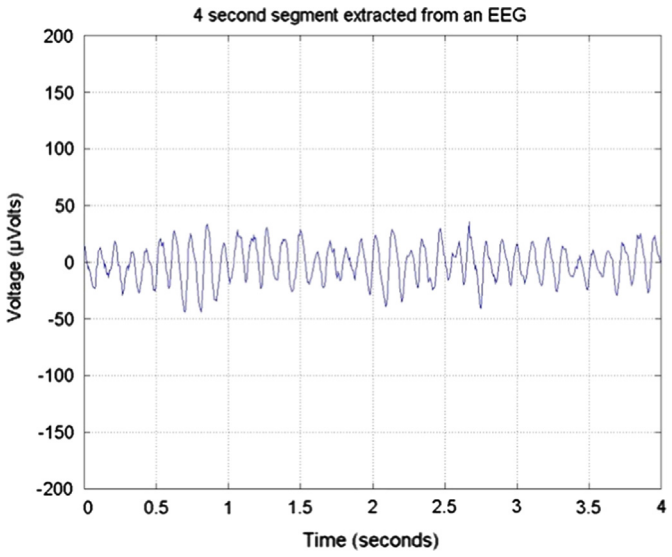

Fig. 1. An example of an EEG waveform.

Support Vector Machines (SVM) classification results based on the above protocols demonstrate the great promise for scalp EEG spectral and complexity features as noninvasive biomarkers for AD early detection.

Artificial intelligence tools have been also widely used to address the problem of AD early detection. In [13], Artificial Neural Network (ANN) was applied to binary AD classification. The protocol of eyes closed subjects is adapted to record EEG waveforms. The implicit function as squashing time (IFAST) based on EEG power spectral density (PSD) and ANN is used for features extraction. Then, a supervised ANN is adopted for binary classification of mild cognitive impairment (MCI) and AD. Experimental results were about 93%.

In [11,14], several techniques a variety of classifiers were tested to perform the task of AD detection in early-stage. The performances of applied techniques are validated thanks to the receiver operating characteristics (ROC). Despite the large number of used methods, results of experiments show that the best classification was about 89%.

In [15], Granger causality, phase synchrony indices, information-theoretic divergence measures, state space based measures, and stochastic event synchrony measures are extracted from healthy participants an AD patients. A comparative study has shown that Granger causality and stochastic event synchrony measures are the best features for AD diagnosis in term of correlation. Experimental results demonstrated that the use of the two selected features has given 83% of good classifications.

In [16], EEG recording process was based on 17 healthy participants and 17 AD patients. The surface topography of the multivariate phase synchronization was analyzed to provide a classification rate of 94%.

Despite its wealth of information, EEG records have been few studied reporting AD classification [13]. Relatively, only few papers discussed the application of EEG datasets for feature extraction, training, classification and validation. In this paper a new approach for the detection of early-stage AD using Simplified Fuzzy Adaptive Theory Map (SFAM) neural network is presented. P300 data were obtained from nine healthy and nine AD subjects as described Jervis et al. in [9,17,18,19]. Using 27 electrodes on the subject scalp, Back-projected independent components (BICs) of P300 peaks are obtained. By combining the ARTMAP-familiarity discrimination (ARTMAP-FD), SFAM neural network and the extracted peaks, AD subjects were separated from healthy ones with a very important accuracy. The proposed methodology is highlighted by an accuracy rate greeter than 95%.

The paper is organized as follows: Section 2 is devoted to the applied methods. In this section, we describe algorithms of independent component analysis (ICA) and Principal Component Analysis (PCA). We define the importance of these techniques for EEG source separation and artifacts removing. The different steps of SFAM neural network are also given in this section. Next, in Section 3, we present a good analysis of the experimental results. The experiment setup and the proposed methodology are also detailed. Section 4 is dedicated to discuss and analyse the experimental results by comparing performances with other approaches. Finally, our conclusions are provided in Section 5.

2. Methods

2.1. Brief description of the independent component analysis technique (ICA)

Independent component analysis (ICA) is one of the most effective signal processing techniques in blind source separation. It can be illustrated with a cocktail party problem where L microphones record the discussion of N peoples whose discuss

together at the same time in groups of various sizes. Each microphone records the superposition of his narrative surroundings. The problem is to find the voice of each person in the dense room getting rid of other voices considered pests. The ICA algorithm is surprisingly robust and its application to solve the superposition of measured EEG waves was often used in scientific papers.

The ICA method is widely used to explore the EEG signals and to estimate the de-mixing matrix W which produces the original sources of the EEG. Following the above definition, the application of the ICA to EEG signals $e_i[n]$ ($e_i[n]=[e_1[n],\ldots,e_L[n]]^T$ $i=1,\ldots,L$, $n=1,\ldots,N$, where L denotes the scalp channels number and N indicates the data points number in the EEG) produces the mutually independent sources $s_i[n]=[s_1[n],\ldots,s_L[n]]^T$ in the matrix form $s=We$ [20].

In order to minimize the mutual information among the data projections, the Infomax ICA algorithm is often used [21]. The major advantage of the Infomax algorithm is the ability to extract noisy activations from non-Gaussian noisy EEG signals. This famous property is validated in [22] where at least 31 separate noisy EEG-like signals were extracted from EEG recordings. Infomax algorithm is talented for extracting noisy activations from non-Gaussian noisy signals [17].

The following assumptions are considered in this work before using the Infomax algorithm [23]:

- The sources are mutually temporally independent;
- The source signals undergo an instantaneous linear mixing to find de-mixing matrix W;
- At most, one of the L sources has a Gaussian distribution;
- The number of measurement channels must be equal to or greater than the number of source signals.

In the next section, the principal component analysis (PCA) is introduced to eliminate the non desired artifacts in recorded EEG signals.

2.2. Principal component analysis (PCA)

In literature, principal component analysis (PCA) is the most used technique for feature reduction which means transforming the original features into a lower dimensional space. PCA, as a linear technique, is a quantitatively rigorous method for achieving data dimensionality reduction of the extracted features. The method generates a new set of variables, called Principal Components (PCs), which maximize the variance of the projected vectors. Each PC is a linear combination of the original variables. All the PCs are orthogonal to each other, so there is no redundant information. The PCs as a whole form an orthogonal basis for the space of the data. Thus, the first PC consists of the highest variability, the second PC consists of the next highest variability and so on for other directions. The first few components are kept and others with less variability are discarded. In this work, the PCA algorithm will be used to eliminate the non significant measures in the recorded EEG signals [24].

2.3. The simplified fuzzy adaptive resonance theory map (SFAM)

2.3.1. Description

The fuzzy adaptive theory map (Fuzzy ARTMAP) is a neural network introduced by Carpenter, Grossberg and Rosen in 1991, which is a modified version of the binary ART [26]. It is notably able to accept analog fuzzy input patterns, i.e. vectors with components between 0 and 1. The Fuzzy ARTMAP is a supervised neural network able of incremental learning, i.e. it can learn continuously without forgetting what it has previously learned [25]. The Simplified Fuzzy

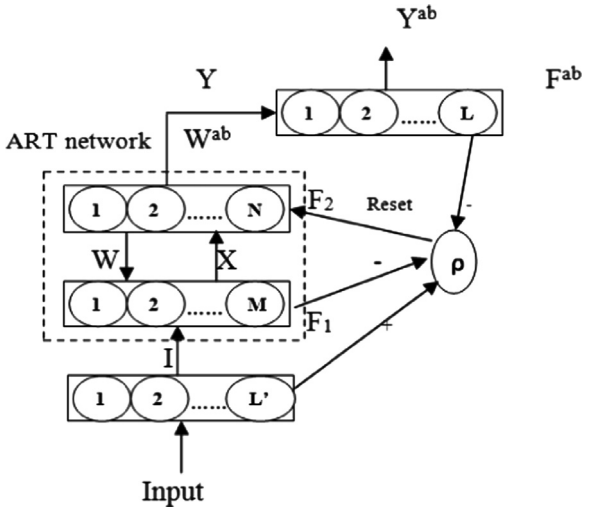

Fig. 2. SFAM network architecture.

ARTMAP (SFAM) neural network is a fast, incremental, supervised learning system for analog inputs. The SFAM network has a simplified architecture when compared to the original Fuzzy ARTMAP [27]. In 1993, Kasuba proposed the SFAM network which is a simplification of Fuzzy ARTMAP [28]. This network is a step ahead of Fuzzy ARTMAP in reducing the computational and architectural redundancy of Fuzzy ARTMAP [28]. Thus, the current study is based on the potential use of SFAM network for the classification process.

The SFAM is formed by three layers of neurons; the input layer F_1, the competitive layer F_2 and the output layer F^{ab} as illustrated in Fig.2.

Both layers F_1 and F_2 have activity patterns, which are fully interconnected. Each neuron is initially connected to every neuron on the other layer. Every connection is weighted between 0 and 1. A neuron of F_2 represents one category formed by the network and it is characterized by its weight vector W_j (j is the index of the neuron). The weight vector's size is equal to the dimension M of layer F_1.

The network uses a form of normalization called complement coding. The operation consists on concatenating the input vector with its complement. The resulting vector is presented to layer F_1. Therefore, the dimension M of layer F_1 is double the input vector's dimension ($M=2L'$).

The F^{ab} layer is connected with the competitive layer F^{ab} by the W^{ab} weights to find the class t of the input vector in the test mode. More details are given in Refs. [29,30].

The different steps of the SFAM algorithm are given in Appendix A.

2.4. Learning process

When an input vector is presented to the network, it is first preprocessed into complement coded form. The resulting vector is called I. The activity pattern on layer F_1 is set equal to I. The choice function is then evaluated for each neuron of F_2. Mathematically, the choice function is defined by:

$$T_j=\frac{\left|I\hat{W}_j\right|}{\alpha+|W_j|} \tag{1}$$

where $|\,.\,|$ is the Euclidian norm, *widehat* is the fuzzy "AND" operator and α is an arbitrary parameter greater than zero which is usually chosen close to zero for a good performance.

Once the winning neuron is selected, a vigilance criterion is evaluated. The vigilance criterion causes the network to choose

another neuron if the first selected is inadequate. Consequently, the vigilance parameter ρ is used to control the SFAM operations.

Mathematically, the vigilance criterion is governed by:

$$\frac{\left|I\hat{W}_j\right|}{|I|} \geq \rho \tag{2}$$

where j is the index of the evaluated neuron in F_2 and ρ is the vigilance parameter, which lies in the interval [0 1].

If the criterion is respected, the SFAM learns the input vector. Contrarily, it selects the next neuron with the uppermost choice function and re-evaluates the vigilance criterion.

These steps are repeated until the vigilance criterion is satisfied. It is then said that the network is in resonance: All F_2 components are set to 0 except the winning neuron which is set to 1.

In the resonance phase, the SFAM proceeds with the input vector I by modifying the weights W_G as follows:

$$W_G^{\text{new}} = \beta(I\hat{W}_G^{\text{old}}) + (1-\beta)W_G^{\text{old}} \tag{3}$$

where, G is the index of the winning neuron and β is the learning rate ($\beta=1$ is used for fast learning mode).

Finally, the Y vector will be send to the map of decision Y^{ab} through the W^{ab} connection to learn associated class already given by the input vector I.

In this paper, SFAM algorithm shows its effectiveness in the classification of the nervous diseases which will be explained herein. Section 3 is dictated to experimental P300 data used for the SFAM classification.

3. Experimental results

3.1. Experimental setup and P300 data recording

Two sets of P300 recordings were performed for nine healthy control subjects and nine confirmed AD patients. The healthy participants (six males, three females) had no history of neurological or psychiatric disorder. They were between 37 and 74 years old. The AD patients (two male, seven female) were between 57 and 88 years old, all with higher education, and were diagnosed with dementia of the Alzheimer's type, in the early stage, mild form, by means of psychometric tests and Cerebral Tomography (CT). They had Mini Mental State Examination (MMSE) scores ranking from 18 to 29, and CT examination showed cortical or cerebral atrophy. Table 1 shows information of healthy participants and AD patients where M (male) and F (female) design the subject's gender, K (unknown), N (no) and Y (yes) are information about subject drug consumption.

P300 evoked potentials were recorded from 27 channels. The electrodes encompassed the largest possible area, recordable from 27 equidistant positions. Linked ears (A_1–A_2) were used as the recording reference and electrode AF_Z was the ground.

Table 1
Information of healthy and AD patients.

Healthy participants				AD patients			
Gender	**Drug**	**Age**	**MMSE**	**Gender**	**Drug**	**Age**	**MMSE**
M	N	37	30	M	K	75	29
F	N	59	30	F	K	73	28
M	N	62	30	F	N	75	29
M	N	62	30	F	Y	78	28
M	N	55	30	F	Y	70	22
F	N	73	30	F	Y	66	18
F	N	74	30	M	Y	88	21
M	N	60	30	F	N	71	29
M	N	60	30	F	N	57	28

The recording cap made by Falk Minow Services, model EASYCAP, and the Large Equidistant 32-Channel-Arrangement, montage No. 23, giving inter-electrode distances of 43 mm to 68 mm (for a head circumference of 58 cm) were used. All EEG electrode impedances were lower than 5 kΩ. The recordings were made using the EMS-GmbH model Phoenix Clinical Lab Digital EEG machine [9]. Following the guidelines in [31], signals were digitally sampled at 1024 Hz, with a high pass filter of cut-off frequency 0.016 Hz, a low pass filter of cut-off frequency 60 Hz, and a notch filter at 50 Hz (to remove electrical mains contamination). Subjects were seated with closed eyes, were relaxed, and were instructed to listen carefully and press a button immediately they heard the target tone.

For each P300 waveform, 599 samples are recorded before the stimulus and 700 samples are recorded after the stimulus. A lot of 1300 samples were derived from any single trial P300. Consider the sampling frequency (1024 Hz), the P300 waveform duration is 1269.5 ms. To have a significant data base, we recorded 40 trials from each subject. Consequently, a total of 720 target trials were recorded (360 from healthy participants and 360 from AD patients). The entire 27 channel measures are back-projected at the Cz electrode.

In [32], authors showed the importance of averaging EPs over trials for increasing the Signal-to-Noise Ratio (SNR). For this reason, we computed the average of the recorded P300 waveforms. By using a random averaging operation for each subject, we have obtained 1175 averaged P300 waveforms from healthy participants and 1419 from AD subjects. We note that for each averaged trial, the number of used single trials is arbitrarily selected between 2 and 40 and it was different from one averaged trial to another. There may be more than 2594 averaged trials but we think that is sufficient for the classification task. Fig. 3 shows an example of an average P300 waveform computed from 19 trials of an AD subject and Table 2 summarizes the number of averaged trials for each subject.

The Signal-to-Noise Ratio (SNR) is defined as the power ratio between the meaningful signal and unwanted noises. To ensure the quality of measures, SNR must reach the largest possible values. To increase SNR, a conventional analysis of AERP is based on synchronized averaging of large numbers of realizations [33]. Motivated by this conclusion, we have averaged the extracted P300 waveforms. The process and method of acquisition of P300 measures are presented in detail in [9,17].

3.2. EEG artefacts removing and features extraction

As a standard pre-processing, PCA algorithm is generally combined within the ICA algorithm. This combination avoids ICA instabilities when the number of samples is limited by reducing the dimensionality of the recorded EEG data [34]. In this paper, the PCA is applied to all single trials P300 waveforms to eliminate the undesired free artefacts. This pre-processing step ensures a faster convergence to the ICA algorithm. Artefacts can be derived ocular artefact, EEGs, algorithmic artefact components, recorded EP…

ICA is very promising for separating out the recorded signals of the temporally independent components, which include electrocardiogram (ECG), ocular artefact, EEG, EP, algorithmic artefact components [35]… By using the PCA method for all recorded EEG single trials, the identification of the EEG signal can be done by canceling undesired signal. This step is generally called “whitening or artefacts rejection”.

As mentioned above, any single trial P300 contains 1300 samples where the stimulus is introduced in the 600th sample. Corresponding to the sampling frequency (1024 Hz) and to the P300 delay (300 ms), the theoretical appearing time of the stimulus should be 885,9375 ms. For this, we applied the PCA

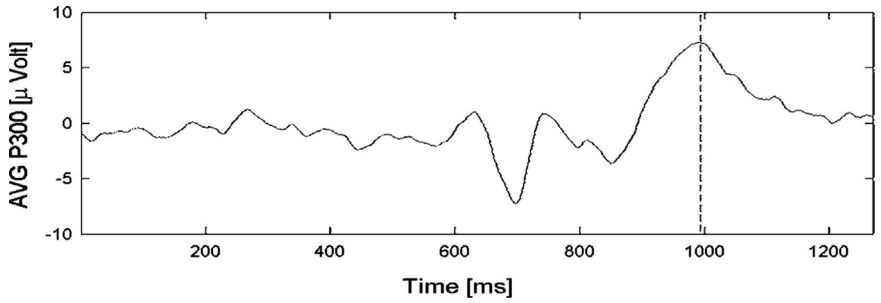

Fig. 3. An example of an averaged P300 waveform.

Table 2
The number of averaged trials computed from healthy and AD patients.

	Healthy participants	AD patients
Subject 1	145	144
Subject 2	136	213
Subject 3	169	177
Subject 4	143	121
Subject 5	128	142
Subject 6	62	169
Subject 7	92	173
Subject 8	174	118
Subject 9	126	162
Total	1175	1419

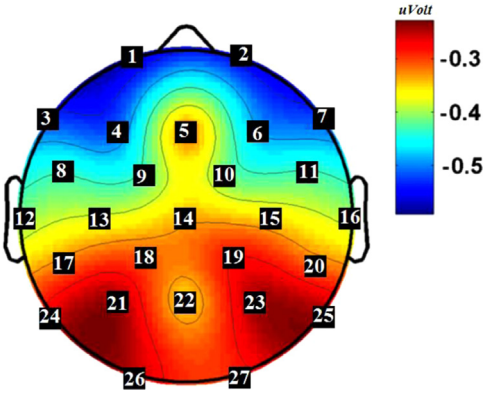

Fig. 4. An example of topography vector for an AD patient and electrode locations.

algorithm in the interval [586 ms1036 ms]. This smart step leads us to reduce the computational time and to cancel all components generated by PCA with low variances which do not traduce stimulus information.

After applying the ICA Infomax algorithm to all whitened and averaged P300 waveforms extracted from healthy participants and AD patients, the 27 components of each averaged trial are obtained. P300 peaks and latencies have been discovered as sensitive markers for AD cognitive dysfunction [36]. Therefore, from the remaining components, the following features were extracted:

- the back projected component peaks (can be negatives or positives);
- the absolute values of the peaks;
- the mean of all peaks;
- the latency time of each peak;
- the mean of latencies.

In [37], it was demonstrated that AD patients exhibited significant decreases of P300 amplitudes. These findings are validated on 31 healthy participants and 31 AD patients. Besides, experimental results in [37] show that there is no significant difference between the two groups in terms of P300 latency. Hence, in this work only the back projected component peaks are used as features and they often known in the literature as "topography vectors" [17]. An image of an extracted topography vector for AD patient and the position of the used electrodes are shown in Fig. 4. The electrode number 14 is the Cz electrode. Fig. 5 shows the feature distribution of 100 averaged trials (50 for healthy participants and 50 for AD patients). From Fig. 5, it is strikingly clear that P300 peaks can easily be separated in two families.

3.3. Correlation study of the extracted features

Alzheimer's disease is a syndrome with multiple etiological factors converged to a loss of essential brain activity synaptic connections. AD etiological factors include genetic abnormalities, cranial trauma, chronic inflammation and mitochondrial dysfunction [2].

Because there is no indication of the etiological factor for the nine AD patients, we have calculated the cross-correlation of each averaged AD trial to get an idea about the correlation of topography vectors. Otherwise, we thought to sub-classify AD's topography vectors for the nine affected cases.

As a powerful tool of signal processing, the cross-correlation has been computed using 1419 feature vectors recorded from nine AD patients. The different necessary steps used in this method are summarized in Table 3.

Note that the cross-correlation coefficient between the selected features vector x and another features vector y of the same AD patient is:

$$CC(x,y) = \frac{C(x,y)}{\sqrt{(Cx,x) \times C(y,y)\,)}} \tag{4}$$

where $C(x,y)$ is the covariance matrix of two vectors x and y.

The study of cross-correlation provides an idea about the degree of similarity between extracted features belonging to the same class (AD subject). Logically, we expect a maximum resemblance to the vectors that belong to the same class, except that in practice only 34% of vectors (overall percentage) are strongly correlated to their classes. The bar chart shown in Fig. 6 clarified the percentage of classification accuracy of all classes.

Fig. 6 shows and confirms that the sub-classification of AD subjects is very difficult. Otherwise, the diagnosis of AD is a hard task. The orthogonality of this work is that it presents a new accurate approach for AD decision making and its early detection which is explained in the next section.

3.4. Proposed methodology for early-stage AD identification

After extracting topography vectors (also called feature vectors) for all averaged measurements, Back-Propagation Neural Network (BPNN) and Probabilistic Neural Network (PNN) are adopted to

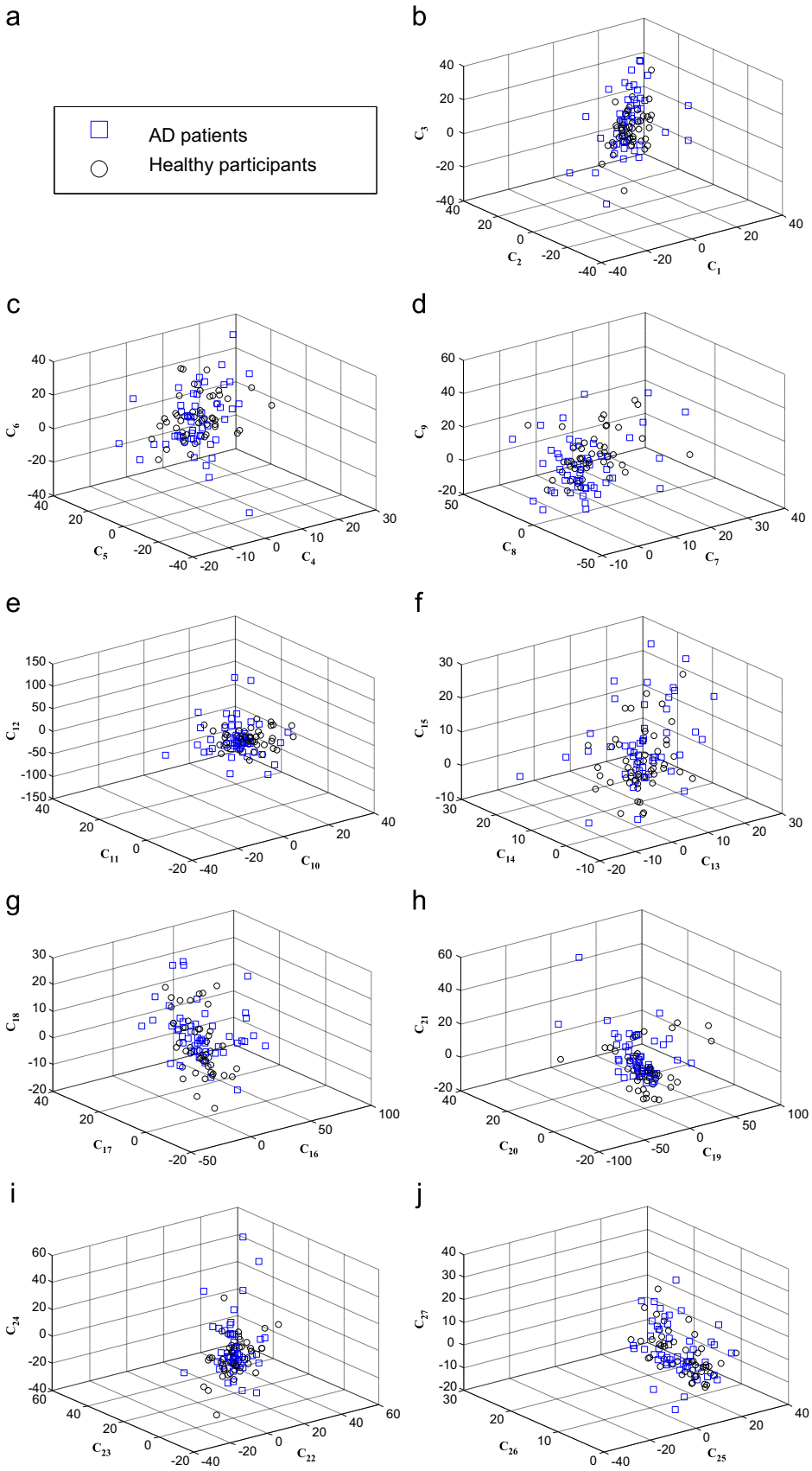

Fig. 5. Original feature distributions: (a) legend, (b) "C_1,C_2,C_3" features, (c) "C_4,C_5,C_6" features, (d) "C_7,C_8,C_9" features, (e) "C_{10},C_{11},C_{12}" features, (f) "C_{13},C_{14},C_{15}" features, (g) "C_{16},C_{17},C_{18}" features, (h) "C_{19},C_{20},C_{21}" features, (i) "C_{22},C_{23},C_{24}" features, (j) "C_{25},C_{26},C_{27}" features.

Table 3
Steps of the proposed cross-correlation algorithm.

Step 1	Select the first class $k=1$ corresponding to the first AD subject
Step 2	Repeat
Step 3	Initialize the classification accuracy $CA_k=0$ of the class k
Step 4	Determine the number of vectors nb_k in the class k
Step 5	Repeat
Step 6	Let y_i a vector from the database ($i=1:nb_k$)
Step 7	Calculate the cross-correlation $CC(y_i,y_i)$ for the vector y_i and all other vectors y_i of the database $j=1:1419\backslash\{i\}$
Step 8	Select the corresponding class to the largest correlation coefficient. If the selected class$=k$ then $CA_k=CA_k+1$
Step 9	$i=i+1$
Step 10	Until $i=nb_k$
Step 11	Calculate the percentage of correct correlations $CCOR\,[\%]=\frac{CA_k}{nb_k}$
Step 12	$k=k+1$
Step 13	Until $k=9$

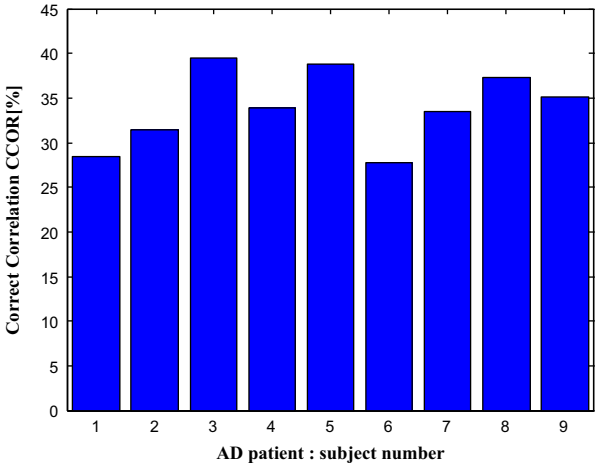

Fig. 6. Percentage of correct correlations for the nine AD cases.

identify the various patterns. The cross-validation method is used to select the optimum proposed neural network structures. The training data set is divided into nine sub-data sets (nine folds). Each fold contains topography vectors recorded from an AD patient and a healthy participant. Then, nine iterations of training and validation are performed. For ach iteration, eight folds are used in the training part and one fold in the validation.

By applying BPNN and PNN, these neural networks were able to identify an overall average Classification Accuracy rate (CA) less than 75%. Compared to previous works, this result is judged as insufficient. Note that CA is the ratio between total numbers of correctly classified test samples to the total number of test samples and it is calculated as follow:

$$CA[\%]=\frac{(number\ \ of\ \ correctly\ \ classified\ \ samples\ )}{(total\ \ number\ \ of\ \ samples\ \ \ in\ \ \ testing\ \ dataset)}100 \qquad (5)$$

Instead of using other intelligent classifier (i.g. Fuzzy Sugeno Classifier (FSC), K-Nearest Neighbor (KNN), Decision tree, SVM…), a new approach of classification is proposed in this paper to ameliorate the previous result. The proposed methodology combines SFAM neural network and ARTMAP-Familiarity Discrimination (ARTMAP-FD) together as follow:

- Apply the SFAM algorithm to sub-classifier AD patients: 1100 vectors are used for the learning phase and the remaining 319 were used in the test phase. The neural network was able to identify all training AD data sets and the overall average classification rate (CA=63.3%) is achieved;
- Identify the winning node G by applying the tested feature vector I to the trained SFAM;

Table 4
Parameters of digital SFAM simulation.

Parameters	Values
L	9
L'	27
M	54
N	700
ρ	0.93
α	10^{-8}
β	1
ε	10^{-5}

- Calculate the ARTMAP-FD for the AD topography vector I as [38]:

$$\varphi(I)=\frac{|I\hat{W}_G|}{|W_G|} \qquad (6)$$

- Identify the familiarity threshold (λ) of the AD class.

Since the nine AD subjects belong to the same class (AD), we were sure that the 1419 extracted AD topography vectors have a common property between them. For these reason we have used the property of the ARTMAP-FD. Hence, experimental results shows that the ARTMAP-FD is often higher than the threshold $\lambda=0.3$. In this way, if $\varphi>\lambda$ we conclude that it is an AD case. Contrary, it is a normal case.

By applying the ARTMAP-FD and the chosen familiarity threshold ($\lambda=0.3$) to the 1175 feature vectors of healthy participants and 319 of AD cases (which are not used in the SFAM learning phase), 95.31% of classification is reached.

We note that the standardization of feature vectors should be done as follows:

- Find the maximum component X_{max} and the minimum component X_{min} for each feature vector I;
- If $X_{max}\geq abs(X_{min})$ then for $i=1:27$ do $X_i=(X_i+X_{max})/(2X_{max})$;
- If $X_{max}<abs(X_{min})$ then for $i=1:27$ do $X_i=(X_i+abs(X_{min}))/(X_{max}+abs(X_{min}))$.

where "*abs*" is the absolute value. In this way, it was possible to have components vectors between 0 and 1. For more details about the SFAM classification, Table 4 provides chosen digital simulation parameters. Note that the choice of vigilance parameter was arbitrary and best results are found in the range of $\rho\epsilon[0.8\ 1]$.

Instead of using a new SFAM network for the identification of early-stage AD with two outputs (the normal case and the AD subject), the ARTMAP-FD is used. Thanks to the structure beyond criticism of SFAM network, we can go even towards 95% of success,

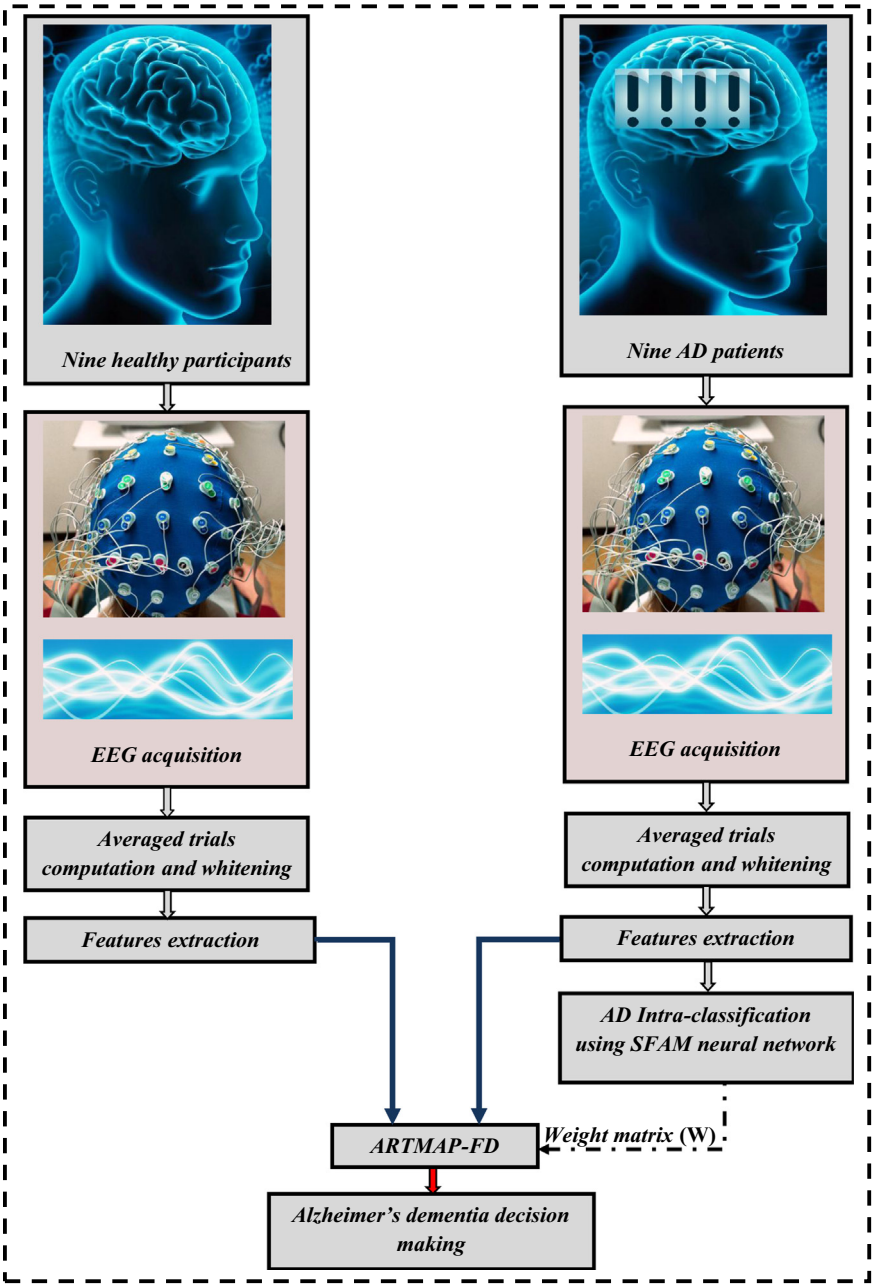

Fig. 7. Proposed diagnostic methodology for AD early detection.

Table 5
Confusion matrix details.

Confusion matrix zone	True positives	True negatives	False positives	False negatives
Term signification	Positive instance classified as positive	Negative instance classified as negative	Negative instance classified as positive	Positive instance classified as negative
AD case	AD case classified as AD	Healthy case classified as healthy	Healthy case classified as AD	AD case classified as healthy
Relation with ARTMAP-FD	AD case and $\varphi > \lambda$	Healthy case and $\varphi \leq \lambda$	Healthy case and $\varphi > \lambda$	AD case and $\varphi \leq \lambda$

even more. The synoptic of the proposed methodology for AD early-stage detection is summarized in Fig. 7.

To improve the CA results and to have more accurate AD diagnosis, we suggest implementing the proposed diagnosis methodology ten times for each subject. Thus, ten topography vectors computed from different ten averaged EEG waveforms of the same subject are used. Consequently, if the diagnosis results show more than five times that it is an AD case, we conclude that it is effectively a subject with AD. Contrary, we conclude efficiently that it is a healthy participant. This smart plan ensures the

precision of the diagnosis result and increase the CA to 100%. Experimental results based on real data from AERP experiments further improve the potential of the proposed analysis framework.

4. Discussion

4.1. Performance evaluation: Need for receiver operating characteristics (ROC) analysis

To validate the proposed combination of SFAM and ARTMAP-FD, receiver operating characteristics (ROC) technique is used. ROC curves are often the only valid method of comparison for methodologies validation and comparison [27]. In biomedical engineering, this technique is often used to demonstrate the quantitative separation effectiveness of the used detectors and classifiers [14].

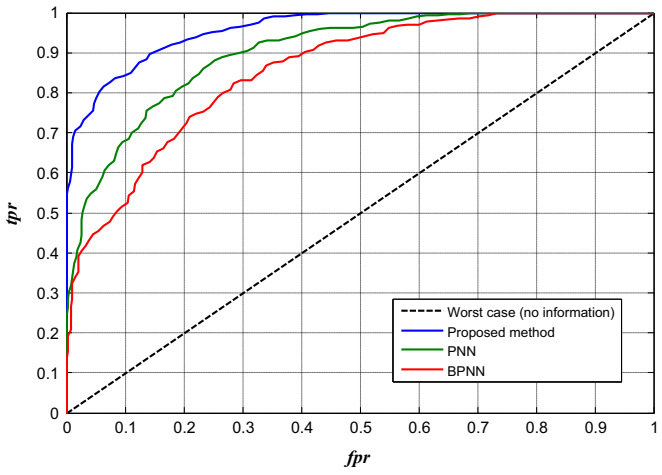

Fig. 8. Comparison of the proposed AD diagnosis methodology versus BPNN and PNN neural networks based on ROC curves.

Following the definition in [27], ROC is very helpful to explore the probability tradeoffs between true positive rates (*tpr*) versus false positive rates (*fpr*). In some literature, *tpr* is called sensitivity and recall and *fpr* is called false alarm. In this work, the four zones of the ROC confusion matrix are summarised in Table 5.

The ROC performance metrics are calculated as follow:

$$tpr = \frac{true\ \ positives}{true\ \ positives\ \ +\ \ false\ \ negatives} \tag{7}$$

$$fpr = \frac{false\ \ positives}{false\ \ positives\ \ +\ \ true\ \ negatives} \tag{8}$$

$$specificity = \frac{true\ \ negatives}{false\ \ positives\ \ +\ \ true\ \ negatives} = 1 - fpr \tag{9}$$

$$specificity = recall \tag{10}$$

To implement the ROC method, random 80 points are selected from the 1494 cases reserved for the test phase (as mentioned above, 319 AD feature vector cases and 1175 feature vectors of healthy participants). This independent Monte-Carlo experiment is repeated 20 times and also 20 ROC curves are obtained. Fig. 8 shows an example of the found ROC curves. Each point in Fig. 8 corresponds to a specific pair of (*fpr*, *tpr*) and the complete curve gives a meaningful overview of the overall performance of the explored test [39]. Fig. 8 proves that the proposed AD detection algorithm is robust in terms of sensitivity and specificity. Compared to BPNN and PNN neural networks, the separation quality of the proposed method is better in terms of sensitivity and specificity: The ROC curve of the proposed method go perfectly from bottom left corner via top left to top right corner. We note that the area under the SFAM ROC curve is bigger that the area of BPNN and PNN ROC curves in the 20 obtained curves. Besides, the SFAM computational time (CPU) is very small compared to BPNN and PNN classifiers. Finally, experimental results show that the proposed combination of SFAM and ARTMAP-FD is a suitable technique for online AD diagnosis. Also, they demonstrate its ability in

Table 6
Comparison of the proposed method with some previous papers.

Literature	Methodology	Accuracy [%]
[12]	– Combination of spectral, entropy and complexity features were tested using SVM classifier	– 79.2% with eyes closed subjects – 83.3% with eyes open subjects – 85.4% with counting eyes closed subjects.
[13]	– MCI and AD classification using IFAST features extraction and supervised ANN classifier	– 91.06% of specificity – 95.87% of sensitivity
[11]	– Several techniques such as, common spatial patterns (CSP), linear discriminant analysis (LDA), spatial filtering, maximum posterior decision rule…	– 88.3% is the best result
[14]	– Features extraction based on spectral power, distribution of spectral power and spatial synchronization – Classification using principal component linear discriminant analysis (PCLDA), partial least squares LDA (PLSLDA), principal component logistic regression (PCLR), partial least squares LR (PLS LR), bagging, random forest, SVM and ANN	– 89% is the best result
[15]	– Two synchrony features: Granger causality and stochastic event synchrony – Linear and quadratic discriminant analysis as a tool of classification	– 89% is the best result
[16]	– Correlation and Linear discriminant analyses of EEG multivariate phase synchronization.	– 94% is the best result
The proposed methodology	– The use of averaged P300 peaks from 27 electrodes as features – Combination of SFAM and ARTMAP-FD as a classification tool	– 95.31% using a single averaged P300 waveform – 100% using ten averaged P300 waveforms

online diagnosing AD with reduced CPU time and significant quality of separation.

4.2. Comparison with some previous works

Classification accuracy is much improved for all AD stages by the use of the EEG features extraction and selection methods. The classification accuracy values are all greater than 75%. Based on these results, it can be concluded that the EEG features extraction methods effectively improve classification performance for the given AD diagnosis task. Table 6 provides a summary of the studies on automated identification of AD. Various expert approaches are tested reporting a CA between 80% and 96%.

In conclusion, the evaluation of our method versus those in previous researches, given in Table 6, highlights our experiment based on P300 peak features, containing non-Gaussian and non-linear information. We suggest that the combination of SFAM and ARTMAP-FD has good potential for improving AD diagnosis. The proposed features with the SFAM classifier produce better classification performance using ten averaged P300 waveforms. The CA result is 95% based on single averaged waveform and the best CA result 100% can be obtained using ten averaged waveforms. The combination of the proposed features and classifier is promising for a high accuracy diagnosis of AD.

5. Conclusion

In this work a new approach for the detection of early-stage AD using SFAM neural network is proposed. Using 27 electrodes for EEG recording, P300 peaks back projected on Cz are extracted from nine healthy participants and nine AD patients. Motivated by the ARTMAP-FD advantages, experimental results show that the proposed combination of SFAM and ARTMAP-FD is very powerful for AD early-stage detection. The proposed method presents many useful characteristics including stability, convergence, and online learning. Compared to some previous works, the proposed method is enhanced in terms of classification accuracy. Finally, the task of AD early-stage detection is really achieved thanks to our proposed methodology.

Acknowledgment

The authors would like to thank Mr. Lotfi Saidi, Ph.D. Student at The University of Tunis, Tunisia, for his pertinent comments to implement the ROC method.

Appendix A

In this section, the different steps of the SFAM algorithm are detailed. To give a rundown of these steps, a meaningful summary is show in Fig. 9.

- Learning mode:
  1. Initialization:
     - All the neurons of F_2 are not made.
     - All the weights in W are set to 1.
     - All the weights in W^{ab} are set to 0.
  2. Encoding of the input vector:
     - Present a vector, a, to the F_0 layer:

$$a = \{a_j \in [01] : i = 1, 2, \ldots, L'\} \tag{A1}$$

     - Coding in complement:

$$I = (a, a_c); \quad a_c = 1 - a \tag{A2}$$

     - The vector I activates the F_1 layer.
  3. Choice of category:
     - The choice function is calculated for each F_2 layer's neuron as:

$$T_j = \frac{\left|I\hat{W}_j\right|}{\alpha + |W_j|} \tag{A3}$$

     - F_2 is a competitive layer where the wining is the neuron G such as:

$$G = argmax\{T_j : j = 1, 2, \ldots, N\} \tag{A4}$$

  4. The vigilance criterion:
     - Compare the similarity between I and W_G on the layer F_1 according to:

$$\frac{|I\hat{W}_G|}{|I|} = \frac{|I\hat{W}_G|}{M} \geq \rho \tag{A5}$$

       - Pass the test: Neuron G is selected and W_G can learn the input I (go to the step 5).
       - Fail the test: Inhibit the neuron G ($T_G = -1$) and return to step 5 to look for another neuron which can pass the test.
  5. Prediction of a class:
     - The code of desired class t is transmitted to F^{ab}.
       - Prediction function: The vector Y activates the F^{ab} layer via the W^{ab} weights:

$$S_G^{ab}(Y) = \sum_{j=1}^{N} (Y_j W_{jG}^{ab}) \tag{A6}$$

       - Prediction:

$$K = argmax\{S_i^{ab}(Y) : i = 1, 2, \ldots, L\} \tag{A7}$$

       - Active for the neuron K corresponding to the prediction ($Y_K^{ab} = 1$and $Y_i^{ab} = 0$ if $i \neq K$);
       - If the prediction K corresponds to the desired class t, go to step 6. Unlike, apply the "match tracking".
       - Match tracking: increase ρ just enough as:

$$\rho = \rho + \varepsilon \tag{A8}$$

       - To find another neuron made of F_2 which predicts the desired class t;
       - To create a new neuron not-clerk of F_2 to learn the desired class if all neurons are tested.
  6. Learning:
     - Update of the prototype G:

$$W_G^{new} = \beta(I\hat{W}_G^{old}) + (1 - \beta)W_G^{old} \tag{A9}$$

     - Create a new associative neuron A if all neurons are inhibited ($W_{At}^{ab} = 1$ where t is the desired class).
- Test mode:
  - Step 2;
  - Step 3;
  - Step 5 (just prediction function and prediction sub-steps); Return to step 2 to take another test.

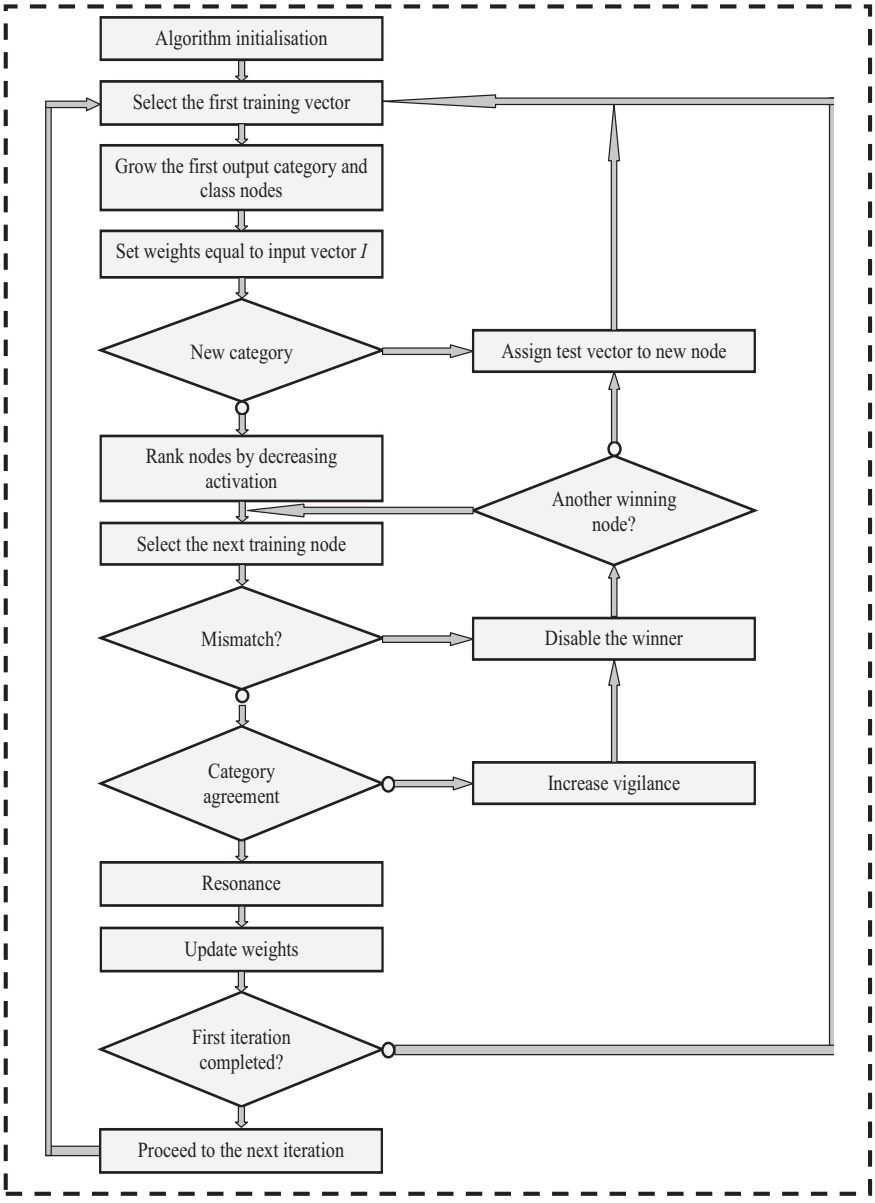

Fig. 9. SFAM flowchart.

References

[1] K. Maurer, S. Volk, H. Gerbaldo, Auguste D and Alzheimer's disease, Lancet 349 (1997) 1546–1549.

[2] J. Villant, Diagnostic de la Maladie d'Alzheimer (et Autres Démences) en Médecine Générale: Évaluation à 6 Mois de l'Impact des Nouvelles Recommandations de la Haute Autorité de Santé, Ph.D. Thesis, University of Paris Descartes, School of Medicine of Paris Descartes, 2009.

[3] J. Hardy, Alzheimer's disease: the amyloid cascade hypothesis: an update and reappraisal, Alzheimers Dis. 9 (2006) 151–153.

[4] M.W. Weiner, D.P. Veitch, P.S. Aisen, L.A. Beckett, N.J. Cairns, R.C. Green, D. Harvey, C.R. Jack, W. Jagust, E. Liu, J.C. Morris, R.C Petersen, A.J Saykin, M.E. Schmidt, L. Shaw, J.A. Siuciak, H. Soares, A.W. Toga, J.Q. Trojanowski, The Alzheimer's disease neuroimaging initiative: a review of papers published since its inception, Azheimer's Dement. 8 (2012) 1–68.

[5] Ph. Scheltens, N. Fox, F. Barkhof, C. De Carli, Structural magnetic resonance imaging in the practical assessment of dementia: beyond exclusion, Lancet Neurol. 1 (2002) 13–21.

[6] R. Oostenveld, P. Praamstra, The five percent electrode system for high-resolution EEG and ERP measurements, Clin. Neurophysiol. 112 (2001) 713–719.

[7] V. Berti, R.S. Osorio, L. Mosconi, Y. Li, S. De Santi, M.J. de Leon, Early detection of Alzheimer's disease with PET imaging, Neurodegener. Dis. 7 (2010) 131–135.

[8] J. Polich, Updating P300: an integrative theory of P3a and P3b, Clin. Neurophysiol. 118 (2007) 2128–2148.

[9] B.W. Jervis, S. Belal, T. Cassar, M. Besleaga, C. Bigan, K. Michalopoulos, M. Zervakis, K. Camilleri, S. Fabri, Waveform analysis of non-oscillatory independent components in single-trial auditory event-related activity in healthy subjects and Alzheimer's disease patients, Curr. Alzheimer Res. 7 (2010) 334–347.

[10] S.A. Hillyard, M. Kutas, Electrophysiology of cognitive processing, Annu. Rev. Psychol. 34 (1983) 33–61.

[11] W.L. Woon, A. Cichocki, F. Vialatte, T. Musha, Techniques for early detection of Alzheimer's disease using spontaneous EEG recordings, Physiol. Meas. 28 (2007) 335–347.

[12] J.C. McBride, et al., Spectral and complexity analysis of scalp EEG characteristics for mild cognitive impairment and early Alzheimer's disease, Comput. Methods Programs Biomed. (2014).

[13] P.M Rossini, M. Buscema, M. Capriotti, E. Grossi, G. Rodriguez, C.D. Percio, C. Babiloni, Is it possible to automatically distinguish resting EEG data of normal elderly vs. mild cognitive impairment subjects with high degree of accuracy? Clin. Neurophysiol. 119 (2008) 1534–1545.

[14] C. Lehmann, T. Koenig, V. Jelic, L. Prichep, R.E. John, L.-O. Wahlund, Y. Dodge, T. Dierks, Application and comparison of classification algorithms for recognition of Alzheimer's disease in electrical brain activity (EEG), J. Neurosci. Methods 161 (2007) 342–350.

[15] J. Dauwels, F. Vialatte, T. Musha, A. Cichocki, A comparative study of synchrony measures for the early diagnosis of Alzheimer's disease based on EEG, NeuroImage 49 (2010) 668–693.
[16] M.G. Knyazeva, M. Jalili, A. Brioschi, I. Bourquin, E. Fornari, M. Hasler, R. Meuli, P. Maeder, J. Ghika, Topography of EEG multivariate phase synchronization in early Alzheimer's disease, Neurobiol. Aging 31 (2010) 1132–1144.
[17] A. Cichockil, R.R. Gharieb, N. Mourad, Extraction of superimposed evoked potentials by combination of independent component analysis and cumulant-based matched filtering, in: Proceedings of the 11th IEEE Signal Processing Workshop on, 237-240, 2001.
[18] B.W. Jervis, S.Y. Belal, K. Camilleri, T. Cassar, S. Fabri, D.E.J. Linden, et al., Comparison of single trial back-projected independent components with the averaged waveform for the extraction of biomarkers of auditory P300 EPs,in: Proceedings of the third International Conference Computational Intelligence in Medicine and Healthcare, CIMED, 2007.
[19] B.W. Jervis, S.Y. Belal, K. Camilleri, T. Cassar, S. Fabri, D.E.J. Linden, et al., Applying ICA to single trial auditory P300 and CNV evoked potentials to provide biomarkers, in: Proceedings of the third International Conference Computational Intelligence in Medicine and Healthcare, CIMED, 2007.
[20] L.D. Lathauwer, B.D. Moor, J. Vandewalle, An introduction to independent component analysis, J. Chemom. 14 (2000) 123–149.
[21] A. Delorme, S Makeig, EEGLAB: an open source toolbox for analysis of single-trial EEG dynamics including independent component analysis, J. Neurosci. Methods 134 (2004) 9–21.
[22] S. Makeig, M. Westerfield, T.-P. Jung, S. Enghoff, J. Townsend, E. Courchesne, T. Sejnowski, Dynamic brain sources of visual evoked potentials, Science 295 (2002) 690–704.
[23] A. Bell, T. Sejnowski, An information-maximization approach to blind separation and blind deconvolution, Neural Comput. 7 (1995) 1129–1159.
[24] K.I. Diamantaras, T. Papadimitriou, Applying PCA neural models for the blind separation of signals, Neurocomputing 73 (2009) 3–9.
[25] G.A. Carpenter, S. Grossberg, A massively parallel architecture for a self-organizing neural pattern recognition machine, Comput. Vision Graphics Image Process. 37 (1987) 54–115.
[26] G.A. Carpenter, S. Grossberg, Pattern Recognition by Self-Organizing Neural Networks, MA: MIT Press, Cambridge, 1991.
[27] T. Fawcett, An introduction to ROC analysis, Pattern Recognit. Lett. 27 (2006) 861–874.
[28] S. Rajasekaran, G. Pai, Image recognition using simplified fuzzy ARTMAP augmented with a moment based feature extractor, Int. J. Pattern Recognit. Artif. Intell. 14 (2000) 1081–1095.
[29] B.W. Jervis, S. Djebali, L. Smaglo, Integrated probabilistic simplified fuzzy ARTMAP, IEE Proc. Sci. Meas. Technol. 151 (2004) 218–228.
[30] B.W. Jervis, T. Garcia, E.P. Giahnakis, The probabilistic simplified fuzzy ARTMAP (PSFAM), IEE Proc. Sci. Meas. Technol. 146 (1999) 165–169.
[31] M.R. Nuwer, G. Comi, R. Emerson, A. Fuglsang-Frederiksen, J.M. Guérit, H. Hinrichs, A. Ikeda, F.J. Luccas, P. Rappelsberger, IFCN standards for digital recording of clinical EEG, Electroencephalogr. Clin. Neurophysiol. 106 (1998) 259–261.
[32] C. Tallon-Baudry, O. Bertrand, Oscillatory gamma activity in humans and its role in object representation, Trends Cogn. Sci. 3 (1999) 151–162.
[33] S. Nishida, M. Nakamura, S. Suwazono, M. Honda, H. Shibasaki, Estimate of physiological variability of peak latency in single sweep P300, Electroencephalogr. Clin. Neurophysiol. 104 (1997) 431–436.
[34] J. Onton, M. Westerfield, J. Townsend, S. Makeig, Imaging human EEG dynamics using independent component analysis, Neurosci. Behav. Rev. 30 (2006) 808–822.
[35] P. Comon, Independent component analysis, a new concept, Signal Process. 36 (1994) 287–314.
[36] J. Polich, Attention, probability, and task demands as determinants of P300 latency from auditory stimuli, Electroencephalogr. Clin. Neurophysiol. 63 (1986) 251–259.
[37] M.-S. Lee, S.-H. Lee, E.-O. Moon, Y.-J. Moon, S. Kim, S.-H. Kim, I.-K. Jung, Neuropsychological correlates of the P300 in patients with Alzheimer's disease, Prog. Neuro-Psychopharmacol. Biol. Psychiatry 40 (2013) 62–69.
[38] G.A. Carpenter, M.A. Rubin, W.W. Streilein, ARTMAP-FD: familiarity discrimination applied to radar target recognition, IEEE Int. Conf. Neural Networks 3 (1997) 1459–1464.
[39] L. Saidi, F. Fnaiech, H. Henao, G.-A. Capolino, G. Cirrincione, Diagnosis of broken-bars fault in induction machines using higher order spectral analysis, ISA Trans. 52 (2013) 140–148.

Jaouher Ben Ali was born in Tunis in 1985. He received the B.Sc. degree in electrical engineering from the Higher School of Sciences and Techniques of Tunis (ESSTT), in 2008 and the M.Sc. degree in automatic control and production engineering, from the same school, in 2011. He is currently working toward the PhD degree in electrical engineering at the University of Tunis. He is a member of research group in Laboratory of Signal Image and Energy Mastery (SIME) of the University of Tunis. His research interest includes application of artificial intelligent and signal processing tools for the diagnosis of nervous diseases and industrial systems.

Sabeur Abid born in 1970 in Sfax (Tunisia). He received the B.Sc. degree in Electrical engineering from the High school of sciences and techniques of Tunis, the DEA degree in Automatic and signal processing from the same school and the Ph.D. degree in signal processing from the National School of engineers of Tunis, respectively in 1993, 1995 and 2002. He is currently an Assistant Professor at the High school of science and techniques of Tunis. Dr. Sabeur Abid has published over 45 scholarly research papers in many journals and international conferences. He was a member of the steering committee of the *IEEE* International Conference on Industrial Technology, 2004, Tunisia. His research interests are focused on Artificial Neural Networks and their applications.

Barrie William Jervis was Professor of Electronic Engineering at Sheffield Hallam University, England, and now works as a consultant. He obtained his B.A. (Hons) and M. A. from the University of Cambridge in Natural Sciences, and his Ph.D. in electronic engineering from the University of Sheffield. He has published more than 50 journal and 60 conference papers, He has delivered more than 40 other technical presentations, and co-authored "Digital Signal Processing: A Practical Approach," and has contributed chapters to 4 other books. His research topics have included semiconductor materials and devices, solid state microwave oscillators and components, microwave instrumentation, the development and application of artificial neural networks to medical data and to fault-finding in electronic circuits, and the determination of gas concentrations in unknown gas mixtures using semiconductor sensors. His current major interest lies in the study of the Independent Components of brain evoked potentials in healthy and Alzheimer's Disease subjects for clinical purposes. He has examined Ph.D. and habilitation theses in Great Britain and France. He has taught communication, electronic, electrical, and microwave engineering, electromagnetic field theory, digital signal processing, expert systems, artificial neural networks, and genetic algorithms. He has worked in the USA, France and Germany, and speaks English, French, German, and Spanish.

Farhat Fnaiech born in 1955 in la Chebba (Tunisia), he received the B.Sc. degree in Mechanical Engineering in 1978 from the High school of sciences and techniques of Tunis and the master degree in 1980, The Ph.D. degree in 1983 from the same school all in Electrical Engineering, and the Doctorate Es Science in Physics form Sciences Faculty of Tunis in 1999. He is currently Professor at the Higher School of Sciences and Techniques of Tunis. Pr Fnaiech is Senior Member IEEE and has published over 170 research papers in many journals and international conferences. He was the general chairman and member of the international Board committee of many International Conferences.

Prof. Fnaiech is associate professor with the Dept of Elect Engineering Higher School of Technologies (ETS) of Montreal Canada and associate researcher with LTI—Univ. of Picardie Jules Verne France. His is Associate Editor of IEEE Transactions Industrial Electronics. He has served as IEEE Chapter committee coordination sub-committee delegate of Africa Region 8. His main interest research areas are nonlinear adaptive Signal processing, nonlinear control of power electronic devices, Digital signal processing, Image Processing, Intelligent techniques and control.

Cristin Bigan is a Professor of Information Technology at Ecological University of Bucharest, Romania. He received Master degree in Electronics and communications and then the Ph.D. in Medical Electronics and Informatics for the Politehnica University of Bucharest. He has published more than 60 journal and conference papers in the field of biomedical signal processing and co-authored 11 books on computer programming and databases. His research interests include EEG and ERP signal processing, classification, event detection and intelligent data processing. He was a researcher participant to the European Biopattern FP6 program.

Mircea Besleaga is a medical doctor, clinician (neurologist) and for many years was the president of the Romanian Society for Clinical Neurophysiology. He was also Romania representative to the International Federation of Clinical Neurophysiology and worked for Bucharest University of Medicine. His current clinical practice at Neuroptics Clinic includes EEG, EMG, ERP. His research interests were on stroke, epilepsy, dementia, EEG and ERP processing. He co-authored over 20 journal and conference papers and 3 books in the field of neurology and was a researcher participant to the European Biopattern FP6 program.